Comparative Analysis of Machine Learning-Based Estimation of Output Current Ripple in PFC-IBC Used in Electrical Vehicle Battery Chargers concerning LR, RF, and ANN Methods

1) SUKURU NAGA SAI SRINIVASU, 2) MUDUNURU RITHIK VAMSI VARMA,

3) GEDALA JAGATH PAVANI, 4) YELAMANCHILI PRIYANKA , 5) PALAKOLLU SAI BALAJI, 6)PAKKI MURARI

1.Student, Electrical and Electrical Engineering , Sanketika vidhya parishad engineering college, Visakhapatnam, Andhra Pradesh

2.Student, Electrical and Electrical Engineering, Sanketika vidhya parishad engineering college, Visakhapatnam, Andhra Pradesh

3.Student, Electrical and Electrical Engineering, Sanketika vidhya parishad engineering college, Visakhapatnam, Andhra Pradesh

4.Student, Electrical and Electrical Engineering, Sanketika vidhya parishad engineering college, Visakhapatnam, Andhra Pradesh

5.Student, Electrical and Electrical Engineering, Sanketika vidhya parishad engineering college, Visakhapatnam, Andhra Pradesh

6.Head of the Department , Electrical and Electrical Engineering, Sanketika vidhya parishad engineering college, Visakhapatnam, Andhra Pradesh

ABSTRACT:

In this study, an artificial neural network (ANN) model is developed based on the inductance current ripple, switching frequency, and load changes to estimate the output current ripple of a power factor correction (PFC) AC/DC interleaved boost converter (IBC) used in battery chargers of electrical vehicles (EVs). Additionally, the enhanced ANN model is contrasted with a few other machines learning (ML) methods, such as random forest (RF) and linear regression (LR). To estimate the output current ripple, the PSIM simulation programme is used to simulate the PFC-IBC. Consequently, 336 output current ripple values are calculated using various switching frequencies, load variations, and inductance current ripple. Next, to manage the current harmonics obtained from the grid and ensure dependable battery charging, the output current ripple value is approximated by training the input parameters using LR, RF, and ANN machine learning methods (MLTs). It may be observed that the estimation value produced by MLTs is rather consistent with the real value that the simulation produced. Furthermore, the simulation-based study requires several days to yield the estimation findings; in contrast, the estimating process using machine learning techniques can be finished in a matter of minutes. This makes the benefit of MLTs very evident. As a result, this value is highly accurately approximated using MLTs prior to the design of the charging apparatus to keep the output current ripple at a safe level, which is crucial for the charging of batteries in electrical vehicles. Additionally, LR, RF, and created ANN approaches were used in this estimating process are looked at and contrasted independently in the WEKA programme, and it is found that the created ANN model offers superior outcomes than alternative methods.

Index Terms: artificial neural network, machine learning, electrical vehicle, power factor adjustment, battery charging.

I. INTRODUCTION

Compared to the vehicles that are commonly used now, internal combustion engines have a more recent history than electrical vehicles (EVs). Because of their poor performance and lengthy charging times, these cars are not being closely researched and are unable to demonstrate advancements during that time [1]. But as alternative energy sources have grown in popularity and laws have been passed to reduce the number of hazardous gases

emitted, interest in EVs has soared once more as fossil fuels have been steadily running out pollution of the environment and atmosphere caused by internal combustion engines.

Electrical vehicle (EV) technology has been evolving in three distinct directions: fuel cell EVs, hybrid EVs, and all-EVs. The batteries that are utilised in car systems and provide chemical energy storage are what unite these three technological advances. Electrical cars must include fast charging capabilities and a long lifespan in addition to high power and energy density for the batteries utilised [2], [3]. One crucial component of electrical vehicles is the battery system. The battery capacity of electrical cars directly affects how far they can travel. Consequently, the requirement for batteries with higher

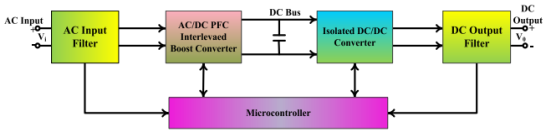

FIGURE 1. The inner structure of a typical switched charger.

The energy capacity is rising steadily. These developments enable the creation of chargers appropriate for the required infrastructure. These days, the charging gadgets usually Ferro-resonant chargers, thyristor chargers, and switching chargers are used on electrical cars. The needs of the application and the battery requirements determine which charging device technology is best. Thyristor and ferro-resonant chargers have a long lifespan and are dependable and robust. However, due to its features such being extremely efficient, lightweight, quiet, low loudness, and quick to react to changes, switched chargers perform better than ferro-resonant and thyristor chargers [3]. The battery charge module, also known as the switched battery charger, is an AC-DC/DC-DC converter with a fully controlled semiconductor power source flip. Due to the ability to manage the MOSFET and IGBT turning on and off, these converters may function at very high frequencies, which results in very low response times for these devices [4]–[6].

A typical switched charger's structure is depicted in Figure 1. The input of the switching charger has an AC filter. The interleaved boost is used to obtain the DC bus voltage. Bridge diodes to correct the AC filter output, resulting in an intermediate-band converter (IBC) at the rectifier's output. An isolated DC-DC converter is used to regulate the DC bus voltage before it is delivered to the output. By modifying and filtering the DC voltage received in the output, the battery is charged. Every step of this procedure results in the generation of the harmonic components.

To ensure the safe charging of electrical car batteries and their extended lifespan, charger output current ripple must be kept at a specific level. When battery chargers have large output current ripples, it causes the batteries overheating and having a shorter lifespan. In actuality, the EV battery would not be fully charged since the battery management system would reduce the charge in the event of overheating. As a result, the vehicle's path will also limit the distance. For these reasons, it is critical to precisely predict the output current ripple value derived from the DC-DC converter output prior to designing and controlling the Machine learning (ML) techniques can now be applied. This is since ML approaches can provide far more useful, quick, and precise solutions in challenging mathematical operations or applications that are challenging to quantify and test. Numerous machine learning (ML) techniques, such as random forest (RF), artificial neural networks (ANN), and linear regression (RL), are available in the literature for use in estimate [8]– [10]. One of the most popular and highly accurate ways is the artificial neural network (ANN) technique [11]– [13].

TABLE 1. List of abbreviations.

ABBREVIATION	DESCRIPTION
EV	Electrical Vehicle
IBC	Interleaved Boost Converter
PFC	Power Factor Correction
ML	Machine Learning
MLT	Machine Learning Techniques
LR	Linear Regression
RF	Random Forest
ANN	Artificial Neural Network
D	Duty Cycle
THD	Total Harmonic Distortion
MLP	Multi-Layer Perceptron
MSE	Mean Square Error
R^2	Correlation Coefficient
MAE	Mean Absolute Error
RMSE	Root Mean Square Error
MAPE	Mean Absolute Percentage Error
MASE	Mean Absolute Scaled Error

An inverter's issue is diagnosed in the research [14] by providing input fault information using machine learning techniques. The study of the IGBT power element's useful life can be found in [15]. The RF approach is used in the study [16] to model a DC-DC converter. As a result, it is observed that the machine learning-based models can offer responses to the simulation findings that are extremely similar. Using the decision tree method, the study [17] estimates the solar panel power needed to connect to the grid. The performance of a soft switched single-phase inverter is investigated in the study [18] because of its ANN control. According to the study [19], the execution of an asymmetric half bridge DC–DC converter with ANN is investigated.

This paper proposes an artificial neural network (ANN) model to estimate the output current ripple of a power factor correction (PFC) - IBC used in electrical car battery chargers, based on variations in frequency, load, and inductance current ripple. The charger's PFC-IBC is a simulation within the PSIM application. As a result of the simulation, 336 data are collected; 315 of these are used to train the network, and 21 of these are used to evaluate the proposed ANN model. It is feasible to reach the estimation results in a lot less time and the findings of the ANN estimation are fairly like those of the simulation. With the created ANN model, this makes it very easy for designers of electrical car battery devices and allows for the provision of an ideal charger design while conserving time. Additionally, using the LR and RF ML techniques in the WEKA programme, all the steps to validate the supplied ANN model are repeated, and the outcomes of these techniques are acquired. A table is used to compare the outcomes of these three machines learning techniques, highlighting the superiority of the suggested artificial neural network model.

II. POWER FACTOR CORRECTION INTERLEAVED AC/DC BOOST CONVERTER

Voltage deformations and current harmonic distortion on electrical systems are significantly increased by the spread of charges, which includes non-linear components like inverters and battery chargers' systems for distributing electricity. Numerous issues, such as excessive neutral currents and power system transformer overheating, may result from these harmonics. AC/DC power converters are utilised in battery charging to reduce these harmonics that are detrimental to the grid and raise the power factor. These converters are favoured as buck, boost, and buck-boost converters. The utilisation of a buck converter in the study suggested in [20] has also been lessened by using greater duty-cycle % variable width PWM signals. In the study suggested in [21], the PFC controller manages the converter's supply current and battery voltage to attain unity power factor. Boost converters are also frequently utilised in addition to these [22], [23]. Depending on the charge, both passive and aggressive approaches are employed and the kind of power factor correction application. Each approach has benefits and drawbacks. To rectify the input current in passive methods, coils and condensers are connected to the rectifier input or output. Despite its straightforward design, this system's usage of grid frequency inductances and capacitances makes it rather unwieldy. Furthermore, this device has a very poor power factor and extremely large non-controlled output voltage ripples [24]. In the active approach that has been thoroughly researched recently, it is attempted to attach a boost DC-DC converter of some kind to the rectifier output to control the output voltage and converge the current towards a sinusoidal shape. The output voltage can also be regulated using a separate circuit [25].

In high power applications, IBC acquired by parallelizing traditional boost converters has been the standard in recent years. In Figure 2's traditional boost converter circuit, the voltage provided to the input is rectified through. By boosting, the rectified voltage and the diode bridge are transmitted to the output. These converters, which are often employed, particularly in PFC applications, are typically run in continuous current mode.

An IBC circuit can be shown in Figure 3 as the converter. In high power applications it is recommended to use an interleaved structure, or parallel operation, of lesser power boost converters to achieve the same power as a single booster converter to employ smaller circuit elements and lessen the high current load on the circuit elements [26].

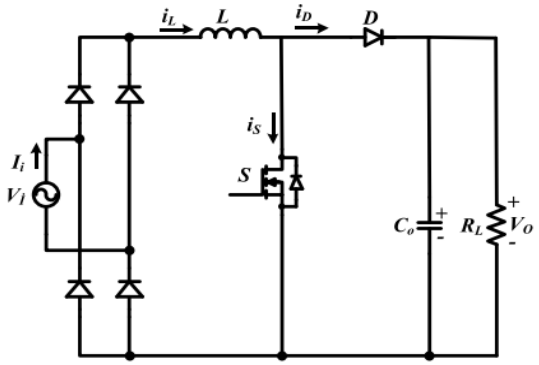

FIGURE 2. The classical boost converter circuit.

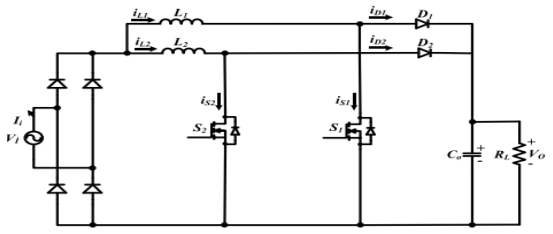

FIGURE 3. The interleaved boost converter circuit.

In comparison to classical boost converters, improved performance can be obtained in operated studies with IBC. This is due to IBC's several benefits, including reduced input. In comparison to conventional boost converters operating at the same power levels, these boost converters feature reduced input filter size, fast transmission responsiveness, ripple free current and output voltage, and little current stress on semiconductor devices [27]–[29].

Input inductance current wave patterns based on having a duty cycle (D) greater or lower than 50% are displayed in Figure 4. One of the main justifications for this study's use of IBC is because of the input current ripple being less than that of a traditional boost converter. As a result, there is less overall harmonic distortion (THD) during battery charging and less current harmonics taken from the grid. The input current ripple is produced by the average of the L1 and L2 inductance currents, as shown in Figure 4. The formulas relating the input and

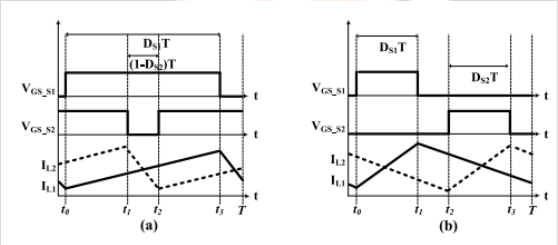

FIGURE 4. Control signals of the switches and the waveforms of boost inductor currents in (a) D > 50% mode, (b) D < 50% mode.

The following output voltages can be supplied for each switch in the converter to indicate whether a switch is turned on or off:

$$\sum_{S_1=on} \Delta i_{L1} = \frac{V_i \cdot (D_{S1}T)}{L_1} \quad (1)$$

$$\sum_{S_1=off} \Delta i_{L1} = \frac{(V_o - V_i) \cdot [1 - (D_{S1}T)]}{L_1} \quad (2)$$

Thus, using equations (1) and (2), the input and output voltage ratio can be obtained as follows:

$$\frac{V_o}{V_i} = \frac{1}{1 - (D_{S1})} \quad (3)$$

III. MACHINE LEARNING (ML) TECHNIQUES-BASED ESTIMATION

The capacity of machines to extract data without explicit programming is known as machine learning. It is a subset or application of artificial intelligence that makes learning possible. Producing a goal-oriented forecast or conclusion in artificial intelligence. Machine learning techniques are used to make. The literature has a wealth of machine learning techniques, some of which include logistic regression, linear regression, simple bayes, k closest

neighbour, random forest, artificial neural network, and decision trees, among others, which are support vector machines.

The machine learning techniques LR, RF, and ANN are applied in this work. The effectiveness of the artificial neural network model created for output current ripple estimate. The LR and RF approaches are contrasted with PFC-IBC, which is utilised in electrical car battery chargers.

A. LINEAR REGRESSION (LR)

An algorithm that is widely used in machine learning and statistics is called linear regression. A desired predictive value is modelled by linear regression using independent variables. The main purpose of it is to determine how variables and predictions relate to one another [9]. Regression models vary in how they depict the connection between the independent and dependent variables factors, as well as the quantity of independent variables employed [30].

The general equation for linear regression is

$$y = c + mx \quad (4)$$

M is the slope, and c is the y-intercept.
The line that fits the body the best is

$$y = mx \quad (5)$$

This equation is commonly represented in statistics as

$$y = \beta_0 + \beta_1 x_1 \quad (6)$$

The equation is if (x1, x2, xn) are the n number of predictors.

$$y = \beta_0 + \beta_1 x_1 + \ldots\ldots\ldots + \beta_n x_n \quad (7)$$

B. RANDOM FOREST (RF)

Like other classification techniques, Random Forest is applied as a supervised machine learning technique for regression and classification. The name implies that it generates a random woodland. Usually, the produced forest consists of a group of decision trees that have been trained using the "bagging" technique. The bagging method aims to improve the overall output by combining many learning models [30].

Overfitting, excessive noise, and outlier issues are not present with RF techniques. In addition, it operates more quickly and produces more accurate results than decision trees and the AdaBoost approach than techniques for boosting and bagging [31]. Due to its many features, including its capacity for multiple regressions and classifications, its speed in the training and testing phases, its ability to handle large data sets, its weighting for various classes, and its visualisation capabilities, the RF technique is a favoured approach [32].

C. ARTIFICAL NEURAL NETWORK (ANN)

An artificial neural network (ANN) is a type of information processing system that has some performance characteristics with biological neural networks and was inspired by them [33]. ANNs, which only mimic the way humans. The brain functions, is capable of generalisation, learning from data, handling an infinite number of variables, etc. It has a lot of significant features.is a potent and versatile data mining technique that may be used to solve difficulties with estimate, classification, and grouping.

The processing element, often known as an artificial neuron, is the smallest unit of an ANN. The five primary parts of the most basic artificial neuron are inputs, weights, coupling function, output, and function of activation. The information that enters the cell from other cells or the outside world is called an input (x1, x2, xn). The examples that the network is asked to learn decide them. The values known as weights (w1, w2, wn) represent how one processing element in the input set or a preceding layer has affected this processing element. Every input is combined using the sum function and then multiplied by the weight that links it to the processing component. The following is the sum function.

$$net = \sum_{i=1}^{n} w_i x_i + b \quad (8)$$

The value obtained from the sum function is passed to calculate the processing element's output.

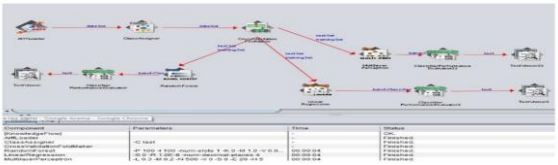

FIGURE 5. The knowledge flow of the used techniques in WEKA.

via a transfer function that is differentiable, either linear or nonlinear.

$$y = f(net) = f\left(\sum_{i=1}^{n} w_i x_i + b\right) \quad (9)$$

This study makes use of an artificial neural network called a multi-layer perceptron (MLP). With one or more layers positioned between the input and output layers, an MLP is a forward-looking neural network. Data travels from the input layer to the output layer in a (forward) direction when it is feedforward. An approach called back propagation learning is used to train this kind of network. MLPs are frequently used for approximation, recognition, prediction, and classification of patterns. Non-linearly separated problems can be solved via MLP. An MLP is a forward-looking neural network with one or more layers situated in between the layers of input and output. Feedforward refers to the movement of data from the input layer to the output layer in a forward direction. Back propagation learning is the algorithm used to train this kind of network. MLPs are frequently used for approximation, recognition, prediction, and classification of patterns. Non-linearly separated problems can be resolved via MLP.

Multilayer neural networks are utilised to solve complicated prediction issues. Because several actions in the hidden layer's structure in these networks have the potential to spontaneously transform into a non-linear composition [34].

The WEKA Explorer module is used in this work to build the three supervised machine learning techniques—LR, RF, and ANN. These methods are models of classification. Ten-fold cross-validation testing is done under the Classify tab of the WEKA Explorer, with a batch size of 100 for all the trials for optimisation. Figure 5 shows the knowledge flow of the employed techniques.

The study's LR, RF, and created ANN model findings are shown according to correlation coefficient (R2), mean square error (MSE), and root mean square error (RMSE), mean absolute scaled error (MASE), mean absolute percentage error (MAPE), and mean absolute error (MAE) measures. The mean square error (MSE) is the result of squaring the difference between the observed and estimated data values in a series and adding the result to the total number of data points. It is a parameter that quadratically indicates the error between the output produced by the prediction model and the desired value. Given that this value was almost zero, it was clear that the predicted value firmly converged to the line. A machine learning model's magnitude of error is measured using the quadratic metric known as root mean square error (RMSE), which is frequently employed to calculate the difference between the predictor's predicted values and the actual values. The standard deviation of the RMSE is estimate mistakes. If the RMSE number is zero, then the model is error-free.

R2 shows how much of the variation in the dependent variable can be accounted for by the independent variable.

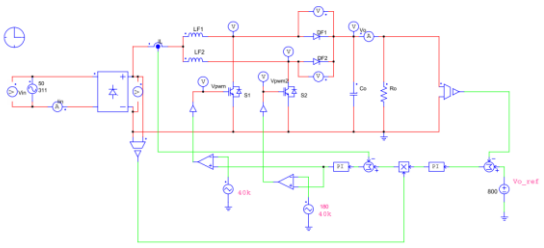

FIGURE 6. Simulation circuit schema and control block of the PFC-IBC converter.

Equation $0 \leq R$ indicates the determination coefficient range, which is equal to the square of the correlation coefficient. $2 \leq 1$. Given that this value is near to 1, it suggests that the independent variable in the model is largely explained by the variance in the dependent variable.

The forecasting model's errors are measured using the MAE, or absolute mean error. It displays the degree to which the estimated and actual values are similar. MAPE refers to the representation of the average absolute error values expressed as a percentage of the real values. The term "high accuracy" refers to estimation models with a MAPE value of less than 10%, whereas the term "accurate estimation" refers to models with a value between 10% and 20%. MASE is calculated by dividing the mean absolute error of the in-sample one-step naive forecast by the mean absolute error of the forecast values. It serves as a gauge for forecast accuracy. When compared to alternative techniques for calculating forecast errors, the mean absolute scale error offers advantageous characteristics, including root mean square deviation, and is thus advised for assessing the relative forecast accuracy [35].

The following equations, in that order, offer the metrics that were employed in this study's evaluation of the estimation findings. The parameters O and P in the equations stand for the observed and expected, respectively.

$$MSE = \frac{1}{n}\sum_{i=1}^{n}(O_i - P_i)^2 \quad (10)$$

$$RMSE = \sqrt{\frac{1}{n}\sum_{i=1}^{n}(O_i - P_i)^2} \quad (11)$$

$$R^2 = \frac{\sum_{i=1}^{n}(O_i - O_{ave})(P_i - P_{ave})}{\sqrt{\sum_{i=1}^{n}(O_i - O_{ave})\sum_{i=1}^{n}(P_i - P_{ave})}} \quad (12)$$

$$MAE = \frac{1}{n}\sum_{i=1}^{n}|O_i - P_i| \quad (13)$$

$$MAPE = \frac{1}{n}\sum_{i=1}^{n}\left|\frac{O_i - P_i}{O_i}\right| \times 100 \quad (14)$$

$$MASE = \frac{\frac{1}{n}\sum_{i=1}^{n}|O_i - P_i|}{\frac{1}{n-1}\sum_{i=2}^{n}|P_i - P_{i-1}|} \quad (15)$$

IV. RESULTS AND DISCUSSION

The PFC-IBC converter utilised in the study is shown by its simulation circuit design in Figure 6, the data for which were taken from the PSIM 9.1.1 programme. The reference measurements made with PI controllers from the input and output are incorporated into the control block to get the control signals for the PFC from the semiconductor power switches in the IBC. The ANN model that was created uses the data from the simulation research that were divided into training and testing sets. The converter's PFC operation is additionally confirmed empirically by setting up an experimental converter circuit prototype. Figure 7 shows a snapshot of the converter's experimental circuit prototype.

The PFC-IBC modelling and experimental findings are displayed in Figure 8. The findings of the simulation and the experimental results are displayed in the figure studies complement one another. The power factor is 0.998, and the waveforms of the input voltage and current are roughly in phase. As a result, the PFC procedure is effective.

When the input parameters are switching frequency (fp), load resistance (RL), and boost inductance current ripple (1IL), the value of output current ripple (1Io) is estimated as the output parameter in this study using a variety of machine learning approaches. Table 2 displays every parameter for both input and output values in the

converter that comprised the methods employed in the simulated study. The switching frequency (fp) in this instance is

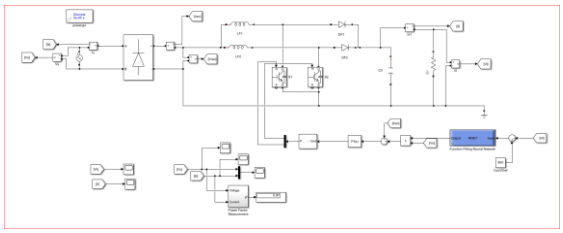

FIGURE 7. The Simulation Implementation of PFC-IBC converter.

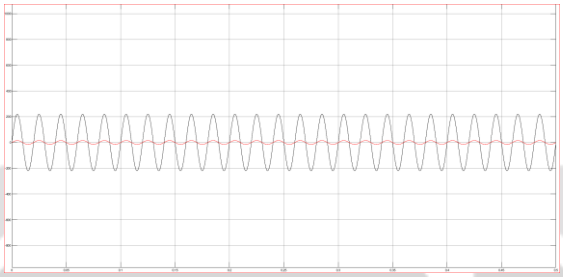

FIGURE 8. The input voltage and current waveforms obtained from a) simulation results

TABLE 2. The parameters of circuit.

Parameter	Symbol	Value
Input Voltage	V_i	220 V_{AC}
Output Voltage	V_O	800 V_{DC}
Output Capacitor	C_o	470 µF
Boost Inductors	L_1, L_2	750 µH
Switching Frequency	f_p	10-40 kHz (Variable in 2 kHz intervals)
Load Resistance	R_L	160-200 Ω (Variable in 2 Ω intervals)

raised in twos between 10 and 40 kHz, and in the data, set used for this investigation, the load resistance (RL) increases in twos between 160 and 200 Ü. As a result, 336 data are derived from simulation overall operation.

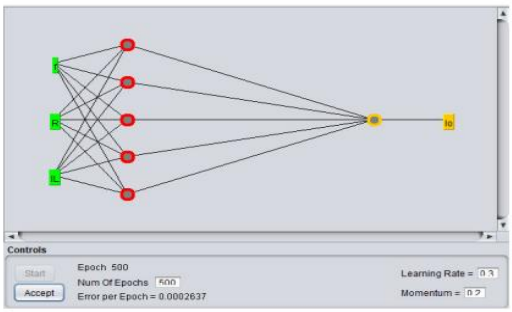

FIGURE 9. ANN model structure for output current ripple.

The ANN model created for the estimation of output current ripple is depicted in Figure 9. As can be observed from the picture, the optimal model developed for the study consisted of a single neural output layer, a five-neural secret layer, and a three-neural input layer.

The actual measurement results and the estimation results coincide in all three ML approaches, as illustrated in Figure, and as a result, it is noticed that the estimation results closely match the genuine results.

V. CONCLUSION

In this work, an artificial neural network (ANN) model is created to estimate, based on the inductance current ripple, switching, the output current ripple of a PFC AC/DC interleaved boost converter used in battery chargers for electrical vehicles. Variations in load and frequency. Additionally, the refined ANN model is contrasted with several machine learning methods, such as random forest and linear regression. Using the PSIM 9.1.1 programme to simulate the converter, the dataset utilised for estimation is obtained. This study uses LR, RF MLTs, and an ANN model that was created for safe battery charging in addition to correcting the power factor and separately estimating the output current ripple. The R2, MSE, and other metrics are used to compare the MLTs estimation results. Performance criteria: RMSE, MAE, MASE, and MAPE. The generated ANN model is found to be more effective than the LR and RF methods. The values of R2, MSE, RMSE, MAE, MASE, and MAPE in the ANN model are computed as follows: 0.995, 0.0006, 0.0245, 0.0002, 0.0714, and 0.2216, in that order. Consequently, the constructed ANN model yields an extremely accurate estimation. To provide dependable charging and a longer battery life for electric vehicle batteries, the output current variation may be predicted thanks to this estimation, which is generated considerably faster than the simulation. This saves charger designers time and convenience.

REFERENCES

[1] J. K. Nor, ‘‘Art of charging electric vehicle batteries,’’ in Proc. WESCON, San Francisco, CA, USA, Sep. 1993, pp. 521–525.

[2] A. Khaliah and Z. Li, ‘‘Battery, ultracapacitor, fuel cell, and hybrid energy storage systems for electric, hybrid electric, fuel cell, and plug-in hybrid electric vehicles: State of the art,’’ IEEE Trans. Veh. Technol., vol. 59, no. 6, pp. 2806–2814, Jul. 2010.

[3] I. A. Khan, ‘‘Battery chargers for electric and hybrid vehicles,’’ in Proc. IEEE Workshop Power Electron. Transp., Oct. 1994, pp. 103–112.

[4] B. J. Masserant and T. A. Stuart, ‘‘A maximum power transfer battery charger for electric vehicles,’’ IEEE Trans. Aerospace. Electron. Syst., vol. 33, no. 3, pp. 930–938, Jul. 1997.

[5] M. M. Morcos, N. G. Dillman, and C. R. Mersman, ‘‘Battery chargers for electric vehicles,’’ IEEE Power Eng. Rev., vol. 20, no. 11, pp. 8–11, Nov. 2000.

[6] C. E. S. Thomas, ‘‘Transportation options in a carbon-constrained world: Hybrids, plug-in hybrids, biofuels, fuel cell electric vehicles, and battery electric vehicles,’’ Int. J. Hydrogen Energy., vol. 34, pp. 9279–9296, Dec. 2009.

[7] V.-S. Nguyen, V.-L. Tran, W. Choi, and D.-W. Kim, ‘‘Analysis of the output ripple of the DC-DC boost charger for li-ion batteries,’’ J. Power Electron., vol. 14, no. 1, pp. 135–142, Jan. 2014.

[8] G. Shanmugasundar, M. Vanitha, R. Cep, V. Kumar, K. Kalita, and M. Ramachandran, ‘‘A comparative study of linear, random forest and ad boost regressions for modelling non-traditional machining,’’ Processes, vol. 9, no. 11, p. 2015, 2021.

[9] K. K. Gupta, K. Kalita, R. K. Ghadami, M. Ramachandran, and X. Z. Gao, ‘‘Machine learning-based predictive modelling of biodiesel production— A comparative perspective,’’ Energies, vol. 14, no. 4, p. 1122, 2021.

[10] O. Arakan, C. C. Uygur, and C. F. Kumu, ‘‘Prediction of dielectric parameters of an aged mv cable: A comparison of curve fitting, decision tree and artificial neural network methods,’’ Electra. Power Syst. Res., vol. 208, Jul. 2022, Art. no. 107892.

[11] A. Anza chi and A. Sarwat, ‘‘Artificial neural network-based duty cycle estimation for maximum power point tracking in photovoltaic systems,’’ in Proc. IEEE Int. Southeast Conf., Fort Lauderdale, FL, USA, Apr. 2015, pp. 1–5.

[12] M. T. Makhloufi, Y. Abdisamad, and M. S. Khairuddin, ‘‘An efficient ANN-based MPPT optimal controller of a DC/DC boost converter for photovoltaic systems,’’ Automatic, vol. 57, no. 1, pp. 109–119, Jan. 2016.

[13] J. N. Marie-Francoise, H. Gallous, and A. Berthon, ‘‘DC to DC converter with neural network control for on-board electrical energy management,’’ in Proc. 4th Int. Power Electron. Motion Control Conf., Xi’an, China, Aug. 2004, pp. 521–525.

[14] S. Khomok and L. M. Tolbert, ‘‘Fault diagnostic system for a multilevel inverter using a neural network,’’ IEEE Trans. Power Electron., vol. 22, no. 3, pp. 1062–1069, May 2007.

[15] A. Aghassi, S. Perinpanayagam, and M. Samie, ‘‘Stochastic RUL calculation enhanced with TDNN-based IGBT failure modelling,’’ IEEE Trans. Rel., vol. 65, no. 2, pp. 558–573, Jun. 2016.

[16] H. S. Krishnamoorthy and T. Narayanan Ayer, ‘‘Machine learning based modelling of power electronic converters,’’ in Proc. IEEE Energy Convers. Conger. Expo. (ECCE), Oct. 2019, pp. 666–672.

[17] J. Wang, P. Li, R. Ran, Y. Che, and Y. Zhou, ‘‘A short-term photovoltaic power prediction model based on the gradient boost decision tree,’’ Appl. Sci., vol. 8, no. 5, p. 689, Apr. 2018.

[18] A. P. N. Ismayil Kani, S. P. B. V. Manikandan, and A. P. K. Premkumar, ‘‘Performance of single-phase soft switching inverter using artificial neural network,’’ Microprocessors Microcyst., to be published, Doi: 10.1016/j.micpro.2021.104236.

[19] A. Gnana Saravanan and M. Rajaram, ‘‘Artificial neural network for monitoring the asymmetric half bridge DC–DC converter,’’ Int. J. Elect. Power Energy Syst., vol. 43, pp. 788–792, Dec. 2012.

[20] S. Das, K. M. Salim, and D. Chowdhury, ‘‘A novel variable width PWM switching based buck converter to control power factor correction phenomenon for an efficacious grid integrated electric vehicle battery charger,’’ in Proc. IEEE Region 10 Conf. (TENCON), Penang, Malaysia, Nov. 2017, pp. 262–267.

[21] S. Kensington and Y. Kumpulan, ‘‘An off-line battery charger based on buck-boost power factor correction converter for plug-in electric vehicles,’’ Energy Proc., vol. 56, pp. 659–666, Jan. 2014.

[22] O. García, J. A. Cobos, R. Prieto, and J. Uceda, ‘‘Single phase power factor correction: A survey,’’ IEEE Trans. Power Electron., vol. 18, no. 3, pp. 749–755, May 2003.

[23] M. Fariborz, E. Wilson, and W. G. Dunford, ‘‘A high-performance single-phase bridgeless interleaved PFC converter for plug-in hybrid electric vehicle battery chargers,’’ IEEE Trans. Ind. Appl., vol. 47, no. 4, pp. 1833–1843, Jul./Aug. 2011.

[24] C. Qiao and K. M. Smedley, ‘‘A topology survey of single-stage power factor corrector with a boost type input-current-shaper,’’ IEEE Trans. Power Electron., vol. 16, no. 3, pp. 360–368, May 2001.

[25] O. Garcia, J. A. Cobos, R. Prieto, P. Alou, and J. Uceda, ‘‘Power factor correction: A survey,’’ in Proc. IEEE 32nd Annu. Power Electron. Spec. Conf., Vancouver, BC, Canada, Jun. 2001, pp. 8–13.

[26] N. S. Ting, Y. Sahin, and I. Aksoy, ‘‘Analysis, design, and implementation of a zero-voltage-transition interleaved boost converter,’’ J. Power Electron., vol. 17, no. 1, pp. 41–55, Jan. 2017.

[27] M. Estelí, B. Poral, E. Adib, and H. Reinhard, ‘‘Interleaved buck converter with continuous input current, extremely low output current ripple, low switching losses, and improved step-down conversion ratio,’’ IEEE Trans. Ind. Electron., vol. 62, no. 8, pp. 4769–4776, Aug. 2015.

[28] M. Estelí, B. Poral, E. Adib, and H. Farzanehfard, ‘‘High step-down interleaved buck converter with low voltage stress,’’ IET Power Electronics., vol. 8, no. 12, pp. 2352–2360, 2015.

[29] K. H. M. S. Chao Yang, ‘‘High step-up interleaved converter with soft-switching using a single auxiliary switch for a fuel cell system,’’ IET Power Electron., vol. 7, no. 11, pp. 2704–2716, Nov. 2014.

[30] A. Dey, ‘‘Machine learning algorithms: A review,’’ Int. J. Compute. Sci. Inf. Technol., vol. 7, no. 3, pp. 1174–1179, 2016.

[31] L. Bierman, ‘‘Random forests,’’ Mach. Learn., vol. 45, no. 1, pp. 5–32, 2001.

[32] A. Cutler, D. R. Cutler, and J. R. Stevens, ‘‘Random forests,’’ Mach. Learn., vol. 45, no. 1, pp. 157–176, 2011.

[33] L. Fausett, Fundamentals of Neural Networks: Architectures, Algorithms and Applications. Upper Saddle River, NJ, USA: Prentice-Hall, 1994.

[34] G. Zhang, B. E. Patio, and M. Y. Hu, ‘‘Forecasting with artificial neural networks: The state of the art,’’ Int. J. Forecasting, vol. 14, pp. 35–62, 1998.

[35] R. J. Hyndman and A. B. Koehler, ‘‘Another look at measures of forecast accuracy,’’ Int. J. Forecasting, vol. 22, no. 4, pp. 679–688, Oct. 2006.